MEMS Technology as Enabler: From Accelerometer to LiDAR

Lj. Ristic,[1] V. Milanović,[1] M. Vujosevic,[2] and A. Kasturi,[1]

[1] Mirrorcle Technologies, Richmond, CA 94804, USA
[2] SensSpree, San Jose, CA 95127, USA

ljr@mirrorcletech.com

Abstract. This paper examines the evolution of Micro-Electro-Mechanical-Systems (MEMS) technology by analyzing high-volume MEMS products introduced over the last several decades. It covers MEMS devices widely used in high-volume applications, as well as MEMS mirrors and their role in optoelectronic applications. The discussion of non-optical MEMS applications highlights well-established products such as accelerometers, pressure sensors, microphones, speakers, and silicon timing devices, each shipping in billions of units annually. The focus then shifts to MEMS mirrors, emphasizing their critical role in opto-electronics. Key applications in this space include vector graphics laser projectors (VGLPs), mixed reality/augmented reality (MR/AR) solutions, free-space optical communication (FSOC), MEMS mirror for optical switching for data centers, and MEMS mirror systems for humanoid robots. Finally, special attention is given to the current state of LiDAR development efforts.

Keywords: MEMS Sensors, MEMS Mirrors, LiDAR, VGLP

1 Introduction

The enormous advances in MEMS sensors made over the last couple of decades and the proliferation of numerous sensor products have been primarily driven by progress in silicon micromachining. Ever since Petersen published his seminal paper on silicon as a mechanical material [1] and Howe and Muller developed polysilicon surface micromachining technology [2], leveraging silicon integrated circuit technology for micromechanical structures has been a focal point for sensor researchers, engineers, and startups. For those interested in exploring the use of silicon and polysilicon in the fabrication of micromechanical structures, references [3,4] provide further insights, while reference [5] discusses how the Complementary Metal Oxide Semiconductor (CMOS) process is being leveraged in micromachining.

The worldwide efforts in this field have not only advanced micromachining but have also established MEMS technology as a mainstream technology that has enabled creation of many diverse sensor products, with billions of units shipped annually. In this paper, we highlight some of these sensor products and discuss the future of MEMS Mirrors.

The paper has two parts. In the first part, we highlight some of the most commercially successful MEMS sensor products, focusing on accelerometers, pressure sensors, microphones, speakers, and silicon timing devices. We describe the key features and technical advances that led to their wide-spread adoption. In the second part of the paper, we explore the optical applications of MEMS Mirrors as a crucial technology in this domain. We discuss several important applications, including VGLP, MR, FCOS, optical switching, and robotics. Finally, particular attention is given to LiDAR and an outline is proposed for its massive adoption.

2 High Volume Applications

The list of MEMS products in high volume manufacturing is rather extensive. However, since the objective of this paper is to highlight exceptionally successful products that have reached mass production, this section will focus only on those that have achieved annual shipment exceeding one billion units. These include accelerometers, pressure sensors, microphones, speakers, and silicon timing devices.

2.1 Accelerometers

Accelerometers were among the first sensors to leverage surface micromachining and successfully be introduced to automotive industry. In the late 1980s and early 1990s, Motorola and Analog Devices led the development of accelerometers for airbag applications. While Analog Devices adopted the comb-structure approach invented by Howe and Lee [6], Motorola pursued a distinct path, developing a three-polysilicon-layer surface micromachining technology and a differential capacitive device as the foundation for its accelerometers [7,8]. Ultimately, both companies were successful in introducing products to automotive customers.

Fig. 1 shows the basic structure of MEMS accelerometer based on differential capacitor developed by Motorola. The device had to satisfy the stringent requirements of the automotive industry: sustaining 1000 g acceleration, incorporating self-test feature and ESD-protection, and being housed in a low-cost hermetic plastic package. All these requirements represented enormous challenges, further compounded by the need to develop a surface micromachining process. Amazingly, all requirements were met. The surface micromachining process with stress-free polysilicon was developed [9], the wafer bonding process was established with a conductive cap [10] to ensure both hermeticity and ESD protection, while a cleverly designed sensing cell took care of self-testing and resilience to high acceleration.

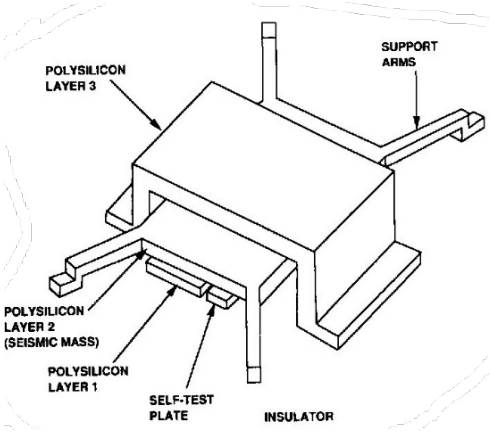

Fig. 1. Polysilicon surface micromachined accelerometer.

The robust capped MEMS accelerometer was ready to be integrated into a plastic package. The final product (Fig. 2) was designed as a two-chip solution where the Integrated Circuit (IC) die accompanied MEMS sensing die in the lead-frame based overmolded package with a built-in stress isolation mechanism [11].

This Motorola's approach enabled a high-yield, high performance, and low-cost solution that was widely accepted by the automotive industry.

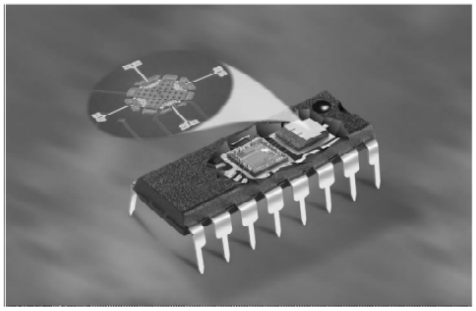

Fig. 2. Motorola accelerometer package for automotive safety application (top mold removed to showcase the IC and MEMS dies, which are mounted side-by-side and electrically connected via wire bonds.) The MEMS die sensing element is also highlighted.

Since the 1990s, MEMS accelerometers have significantly expanded their range of applications. Advances in miniaturization, high-yield manufacturing, and cost-effective production have driven their continued growth in the automotive market and facilitated their widespread adoption across new markets, including consumer electronics, industrial automation, robotics, medical devices, the Internet of Things (IoT), and defense. Today, MEMS accelerometers play a crucial role in applications such screen orientation

detection, movement monitoring, step counting, gesture recognition, structural health monitoring, and vibration monitoring of machinery, among many others.

2.2 Pressure Sensors

Pressure sensors are devices that convert mechanical pressure into an electrical signal. A key component of every MEMS pressure sensor is a diaphragm. There are various manufacturing techniques for fabricating silicon diaphragms [3,4,12]. The chosen technique is primarily determined by the sensor's underlying operating principle.

Generally, two fundamental principles are exploited in MEMS pressure sensors: the piezoresistive effect [13] and the capacitive sensing [14]. In the case of the piezoresistive effect, a piezoresistor is embedded within the diaphragm. When the diaphragm deforms due to pressure changes, the resulting strain alters the resistance of the piezoresistor, which is then correlated to the pressure. In capacitive sensing, the diaphragm itself serves as one electrode of a capacitor. Changes in pressure cause diaphragm movement, altering the capacitance, which is then used to determine the pressure variation.

Piezoresistive Pressure Sensors. In this approach, a silicon diaphragm is fabricated in silicon crystal using wet anisotropic etching of a silicon wafer with a (100) orientation. The bulk micromachining process leverages the fact that silicon crystallographic planes with a (111) orientation etch at a significantly slower rate than those with a (100) orientation [15-17]. This results in a characteristic sloped, truncated pyramidal cavity beneath the diaphragm (Fig. 3a).

Piezoresistive resistors are strategically placed at the edges of the diaphragm to maximize sensitivity, as these areas experience the highest stress during membrane bending. The piezoresistor requires a special design, such as the X-ducer used in Motorola pressure sensor [18], or the Wheatstone Bridge configuration used by STM [19]. Once the sensing element is fabricated, the MEMS wafer is bonded to a holder wafer, creating a sealed cavity (reference chamber) for absolute pressure sensing. This approach has been widely adopted by many pressure sensor manufacturers.

The next step is packaging. Unique packaging schemes for pressure sensor devices enable a wide range of applications, from absolute pressure measurement to differential pressure sensing. Over the years, MEMS pressure sensor packaging technology has evolved, developing various types of packaging schemes to protect the die while allowing exposure to the environment. In addition to protection from thermomechanical stresses, specific shielding features against chemically aggressive environments have been critical for expanding into new markets, including automotive, industrial, consumer, and medical [20]. The complexity increases for certain applications that require specialized materials — for example, white plastic based polysulfon is used in medical devices for its chemical resistance and biocompatibility [21].

Capacitive Pressure Sensors. In the case of capacitive pressure sensor, a surface micromachining is used in combination with a thin polysilicon layer and sacrificial etching. The sensor features a sealed cavity and a thin diaphragm, which also functions as

one of the capacitor plates (Fig. 3b). The pressure sensor sits on the top of the MEMS die. This technology is extensively used for making high-pressure sensors. Capacitive pressure sensors form the core of Tire Pressure Monitoring Systems (TPMS) [22]. A notable example is Freescale's TPMS solution, which integrates a capacitive pressure sensor, accelerometer, temperature sensor, integrated MCU, 16 kilobytes of RAM, low-frequency receiver, and high-frequency transmitter, all in a Single inline Package (SiP) [23]. Accelerometer turns off the device when vehicle is still, but also records acceleration when moving. Pressure sensor measures tire pressure, while temperature sensor records temperature for data correlation. LF receiver serves for programing and resetting, while HF transmitter transmits data for warning and data analytics. This product has become a cornerstone in the automotive industry, widely used in both passenger vehicles and commercial trucks for real-time tire pressure monitoring.

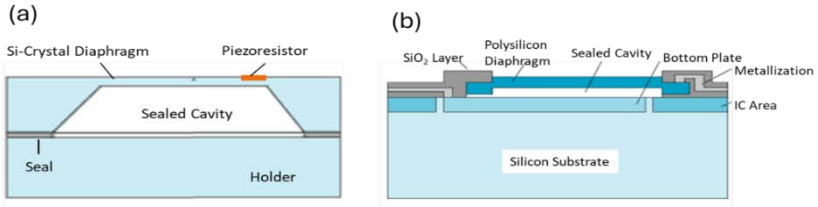

Fig. 3. (a) Piezoresistive pressure sensor fabricated using wet anisotropic etch; (b) Capacitive pressure sensor fabricated using surface micromachining.

2.3 Microphones

A MEMS microphone is an acoustic sensor that converts sound into an electrical signal. There are different types of MEMS microphone technologies [24], but the most dominant type is capacitive MEM microphone which account for 80% of the market. The basic structure of a capacitive MEMS microphone is shown in Fig. 4. [25]. It consists of a very thin diaphragm and a backplate. The sound wave creates air pressure that moves the diaphragm relative to the fixed backplate. The resulting change in capacitance between the diaphragm and the backplate is converted into an electrical signal and processed by an ASIC. The ASIC die is a separate die that, together with the MEMS die, is placed within the same package.

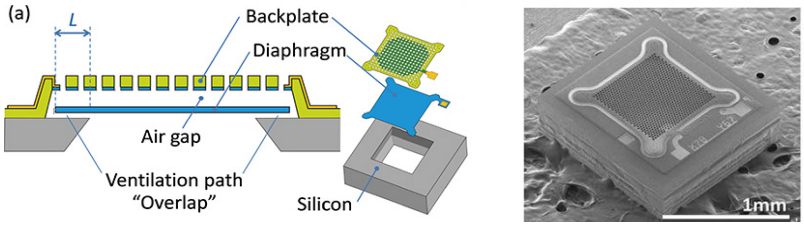

Fig. 4. MEMS microphone: (a) cross-section, (b) SEM image.

A MEMS microphone module is an open-cavity package in which MEMS die and ASIC die are placed side by side on an organic or ceramic substrate and connected via

wire bonding. The package includes a sound port that allows sound to enter. This port is often located in the package substrate creating a bottom-port configuration (Fig. 5) [25], but it can also be placed in the lid for a top-port design. The port's location is determined by the integration and placement requirement of the MEMS microphone module within the final system.

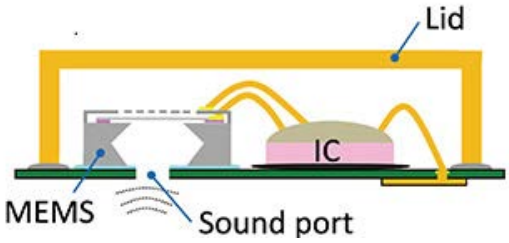

Fig. 5. Microphone module – schematic representation.

Microphones have significantly benefited from ongoing advancements in MEMS technology, leading to substantial miniaturization of these devices. As a result of their small size and low power consumption, MEMS microphones are well-suited for applications in compact, battery-powered devices such as smartphones, tablets, smartwatches, earbuds, hearing aids, laptops, smart speakers, etc. Additionally, new use cases for these devices have very recently driven the development of more environmentally robust technologies, as discussed in [26-28]. The maturity of the technology and its low cost have made MEMS microphones ubiquitous. Moreover, this advancement has transformed how people interact with modern devices, as evident by the widespread adoption of voice control and hands-free communication.

2.4 Speakers

A MEMS speaker produces sound by converting an electrical audio signal into a sound wave using MEMS technology. At its core, the speaker features a diaphragm whose vibrations move the air in the air chamber creating sound. High quality sound generation requires significant movement of the diaphragm. Unlike MEMS microphones that necessitate a very small diaphragm displacements, MEMS speakers require larger diaphragm motion to effectively move air and produce sound.

There are four basic transduction principles used to drive the diaphragm: piezoelectric [29], electrodynamic [30], electrostatic [31], and thermoacoustic [32]. An excellent review of these driving mechanisms can be found in [33]. Currently, piezoelectric MEMS speakers dominate the market. Therefore, as an example, we here briefly describe only the piezoelectric MEMS speaker (Fig. 6) [33].

MEMS speakers are typically designed to operate within a frequency range of 20 Hz to 20 kHz, aligning with the human hearing range. However, in daily life, most audible sounds range from 100 Hz to 10 kHz, including speech (primarily 300 Hz–3.4

kHz) and musical harmonics (extending beyond 6 kHz). Due to the small size and limited diaphragm movement of MEMS speakers, their low-frequency response is often a challenge. Therefore, it is a must to evaluate MEMS speakers across both low-frequency and high-frequency bands.

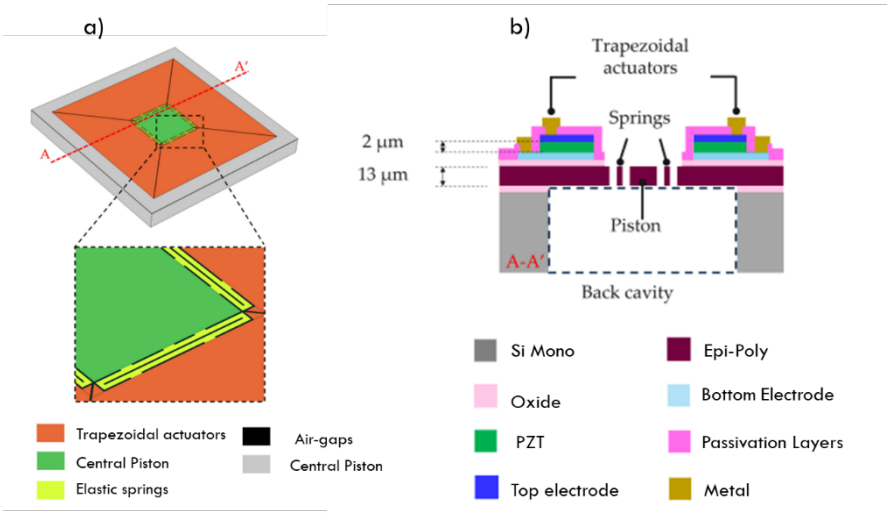

Fig. 6. a) Top view of speaker diaphragm, b) Cross-section of speaker diaphragm.

MEMS speakers are among the most recent product families to leverage MEMS technology, with commercial products emerging only over the last decade. Their development has generally been more challenging compared to MEMS microphones. This challenge is primarily driven by the need for large diaphragm displacement, as mentioned earlier. On one hand, sufficient power is required to generate enough force to move the diaphragm, while on the other hand, the structural integrity of the diaphragm must be preserved despite large displacements and sustained high stresses.

The advantages of MEMS speakers over traditional non-MEMS technologies (such as electrodynamic and balanced armature speakers) are their small form factor, lower power consumption, batch fabrication, and ease of integration with electronics. These benefits make them highly attractive for many applications in consumer electronics and other size- and power-constraint applications.

2.5 Silicon Timing Devices

The main purpose of MEMS timing devices is to provide clock functions that are required in modern electronic products. The frequency range of these devices spans from Hz to MHz and they offer programmability. They are an excellent alternative to crystal oscillators and are gaining acceptance in many market segments including automotive, aerospace and defense, telecommunications, IT, consumer, and medical applications. They offer reliable performance, low power consumption, high stability, small form factors, and low cost.

There are three main categories of MEMS timing devices: resonators, oscillators, and clocks [34,35]. Typically, silicon resonators are designed as devices that serve as the source of frequency, while oscillators include resonator and ASIC to drive it and compensate performance of resonator and make it continuous and stable. Finally, clocks often combine multiple oscillators to create source of multiple reference frequencies.

All commercial silicon MEMS resonators are based on electrostatic driving mechanism. A cross-section example of a resonator developed by Si Time is shown in Fig. 7. [36]. The resonator is etched in silicon on the insulator layer. Since silicon is a stable material, the resonator exhibits high quality factors and near zero frequency drift. The resonator is sealed at the wafer level [36,37] using high-temperature polysilicon deposition to create a clean vacuum environment needed for stability.

The resonator is then assembled in a single package together with a COMS ASIC to form an oscillator. The resonator and ASIC are integrated as a die stack within a plastic package. The ASIC itself represents an art on its own and includes resonator sustaining circuit, charge pump, fractional-N PLL, temperature sensor with digital temperature compensation, non-volatile memory, as well as output dividers and drivers. The final result is an outstanding performance 20 MHz MEMS oscillator with a stability of ± 25 ppm [36].

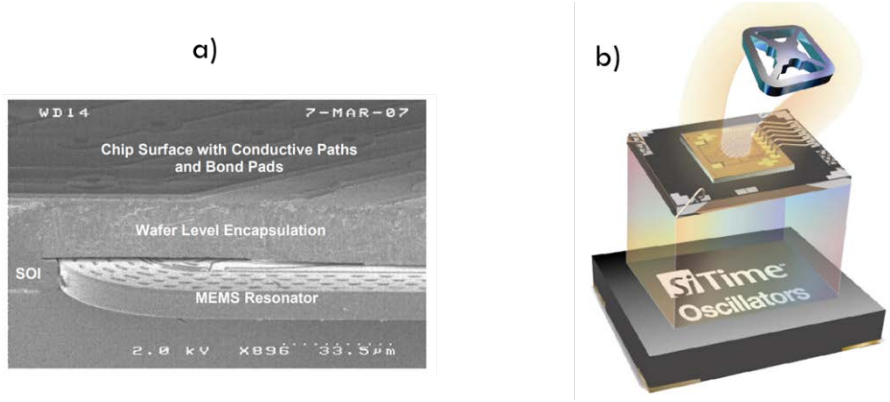

Fig. 7. a) Silicon MEMS Resonator, b) Silicon MEMS oscillator.

3 MEMS Mirror – Essential Device for Photonics Applications

MEMS Mirrors are small silicon-based devices capable of tilting along a single axis (one-dimensional mirror) or in two axes (two-dimensional mirror) [38,39]. Depending on the design they can also move along a third axis making a piston action [38]. Usually, MEMS mirrors are made in a circular shape with diameters ranging from 0.5 mm to 10 mm [40].

The technology for making MEMS mirrors has significantly matured over the last two decades. Today, three primary actuation principles are used to make MEMS

mirrors move: electrostatic, electromagnetic, and piezoelectric actuation. A comparative summary of these approaches is shown in (Table 1). Each method has its own advantages and limitations, determining their suitability for different applications.

Silicon is the core material used for making MEMS mirrors across all three actuation techniques, though some methods require additional material to enable mirrors movement. For example, electromagnetic actuation requires use of additional magnets, while piezoelectric driving requires lead zirconate titanate (PZT) films. Designers must make trade-offs between key performance parameters to select the most suitable MEMS mirror for a given application.

Table 1. A comparative summary of basic parameters between electrostatically driven, electromagnetically driven, and piezoelectrically driven MEMS mirrors**.**

Parameters	Electrostatic Driving	Electromagnetic Driving	Piezoelectric Driving
Core Material	Si	Si	Si
Additional Material	n/a	external magnets	PZT + passivation
Power Consumption	< 1 mW	~ 500 mW	~100 mW
Drive Voltage	high	low	high
Drive Current	very low	high	medium
Temperature Sensitivity	low	high	high
Hysteresis	none	medium	high
Deflection Angle (linear)	(+/-) 7.5 deg	(+/-) 15 deg	(+/-) 15 deg
Device Manufacture	standard IC process	IC + added complexity	IC + added complexity
Electronic Control	simple	medium	closed loop required
Non-resonant Mode	yes	yes	no
Resonant Mode	yes	yes	yes
Vector Graphic Mode	yes	yes	yes
Size	smallest	largest	medium

Examples of different MEMS mirrors are shown in Table 2 [41]. The device diversity offered in various sizes and packages demonstrate that MEMS Mirror technology has reached a high level of maturity.

Table 2. Dual-axis Quasistatic MEMS mirrors ranging from 2 mm to 6.4 mm in diameter.

		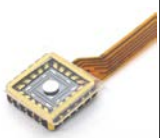 Compact package, <0.4g mass	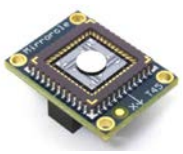	 Hermetic package, 2.5g mass
MEMS Mirror	A7M20.2-2000AL	A7B1.3-2400AL	A8L2.2-4200AL	A5L3.3-6400AL
Package and Cover	TINY48.4-NW	LCC20-TW	TINY48.4-NW	TO8-CAPSC1
Mirror Diameter	2.0mm	2.4mm	4.2mm	6.4mm
Optical Angle	±10°	±16°	±11°	±5°
First Resonance	1300Hz	600Hz	450Hz	300Hz
Feature	high bandwidth	large angle	large angle*diameter	large diameter

3.1 MEMS Mirror Basic Function and Scanning Engine

A MEMS mirror's primary function is to deflect a focused beam of light in different directions. The light beam can be steered along a single axis (one-dimensional mirror) or along two axes (two-dimensional mirror). This ability to receive and redirect a focused beam of light is fundamental to scanning technology.

In an electrostatically driven mirror, tilting occurs when a voltage is applied to a set of comb-finger electrodes. A 1D mirror has one set of electrodes on opposite sides of the mirror, while a 2D mirror has two sets of electrodes for independent movement along both axes. Fig. 8 shows MEMS Mirror with two pairs of comb-drives [38], one pair for each axis. These electro-static actuators (comb-drives) are an integral part of the MEMS mirror device, whereas the electronic circuit that controls the tilting is a separate IC.

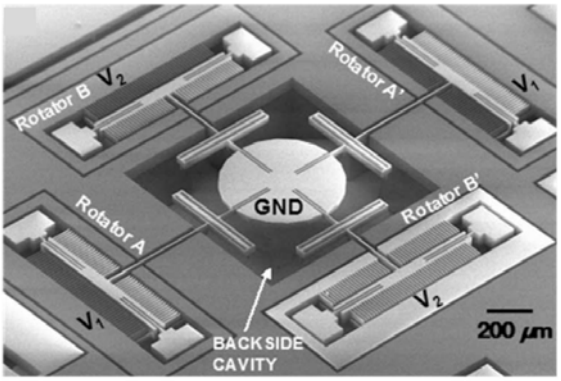

Fig. 8. SEM of an early demonstration of 2D-MEMS Mirror with two pairs of comb-drives and gimbal-less structure allowing efficient dual-axis tip/tilt as well as piston actuation. Comb-drive pair A-A' tilts mirror along x-axis, and pair B-B' tilts mirror along y-axis.

The device architecture shown above is the essential modular building block for a portfolio of MEMS mirrors with optimization for different use cases and applications. The architecture covers cases for single- and dual-axis actuation, resonant and broadband (quasi-static) actuation, as well as different mirror sizes and coatings.

The scanning capability of MEMS mirrors is cleverly utilized to enable two basic functions for manipulating laser light: directed light projection and directed light acquisition (imaging). There are applications that utilize either functionality and some applications in fact utilize both projection and imaging (e.g. LiDAR). In the following sections we describe multiple applications of MEMS mirror-based systems, and then we pay special attention to LiDAR technology.

3.2 Vector Graphics Laser Projector and Applications

Laser projectors convert moving light into higher-level information such as signs, graphics, and videos. Visual information can be presented using several methods,

including Vector Graphics Laser Projection (VGLP) mode, raster mode, and Lissajous mode. MEMS-based VGLP (MEMS VGLP) is currently a topic of great interest due to its ability to produce high-brightness images even in outdoor daylight conditions. In this paper, we focus exclusively on the MEMS VGLP method.

MEMS VGLP enables compact pocket-size projectors capable of providing high brightness visual messaging in daylight environment on multitude of different surfaces. The key differentiation compared to other projection technologies is its VGLP concept, which enables superior high-brightness performance. A distinguished product in this category is branded as Playzer by Mirrorcle Technologies [42,43]. A high-level block diagram of this device is shown in Fig. 9.

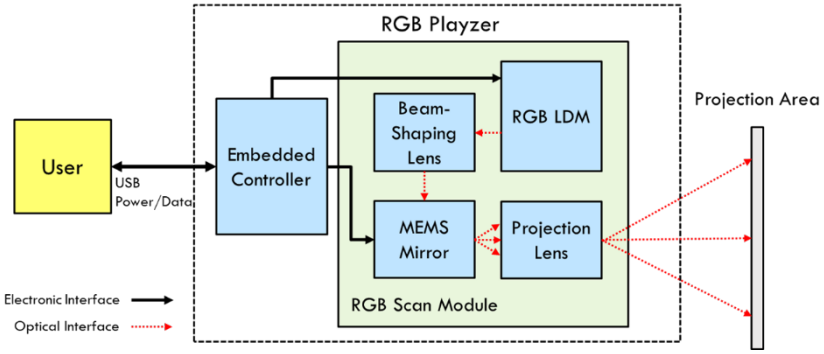

Fig. 9. Playzer - high level architecture.

The hardware consists of a MEMS mirror, one or more lasers, optics, and electronics. An essential part of this product is its software. The RGB laser diode module (RGB LDM) serves as the light source, generating one or more laser beams that are optically focused by a beam-shaping lens and directed toward the MEMS mirror. The mirror steers the beam in different directions to create the desired message in the form of graphics or text. Both the RGB LDM and the MEMS mirror are controlled by integrated electronics and software.

Monochrome Playzer version has been implemented with different laser wavelengths, particularly in four different colors (red, green, blue, and violet). Laser intensity or brightness of the vector graphics is controlled by a laser driver which allows 256-levels of control within content data but also has programmable gain and offset to calibrate to each laser diode and modulate based on environmental conditions. On the other hand, RGB Playzer includes 3 laser sources (red, green, blue) and is a full color projector (256 x 256 x 256 colors). It is integrated into a small box, approximately 90 cm3, weighing under 200g, and consuming less than 2W of power. Notably, the majority of the power is consumed by lasers. The Playzer is programmable, allowing for the creation of customized messaging tailored to specific applications. Several examples of the Playzer in action are shown in Fig. 10. Fig. 10a is an example of MEMS mirrors used for video projection at video-raster rates (720p in this example). This produces color-rich imagery and videos, however with very limited brightness which practically limits

the use of technology to dark environments and short distance projection. In contrast Fig. 10b shows RGB Playzer with same RGB laser capability and similar MEMS Mirrors but due to the VGLP nature of projection it is projecting bright content at a building wall more than 10m away and during daytime (shaded side of building). Other examples illustrate various automotive applications of MEMS mirror based VGLP such as head up display (HUD) in Fig.10c, programmable courtesy lighting in Fig.10d and 10e, and programmable headlights (prototype dynamic laser lighting projector in Fig. 10f projects programmable white vector content onto a building at >10m distance).

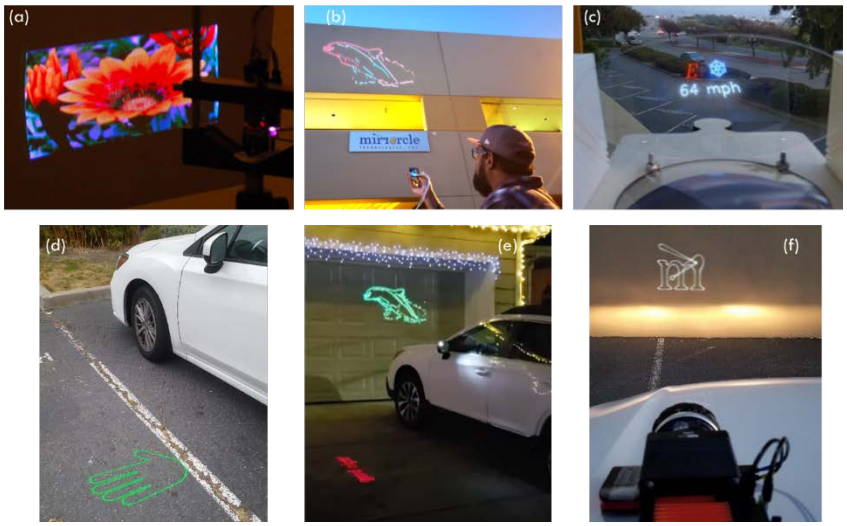

Fig. 10. a) MEMS raster projector, b) RGB Playzer in VGLP mode, c) VGLP HUD display, d) VGLP courtesy lighting – projection om the concrete, e) VGLP courtesy lighting projection on the wall, f) dynamic laser light projector – white VGLP projection on a wall

Applications for VGLP are numerous and include automotive, agriculture, robotics, MR, commercial, consumer, industrial, transportation, and smart city markets.

3.3 Mixed Reality (MR) Applications

Augmented Reality (AR) is a term that began gaining traction in the late 1990s [44,45] to describe systems designed to enhance user perception of the real world by supplementing it with 3D virtual objects that coexist within the same space as the physical world. The existence of virtual objects led to the term Virtual Reality (VR), while the blending of real and virtual objects gave rise to the term Mixed Reality (MR). These terms are often used interchangeably to describe systems that merge with real and virtual environment and allow for real-time interaction. In this paper, we will use the term *Mixed Reality (MR).*

It is important to note that MR is not limited to specific display technologies or to visual perception alone —it applies across all human senses. Over the past two decades, there has been enormous effort and investment in developing MR technology and

products. These efforts can be broadly categorized into two major areas: 1) Immersive MR, featuring head-mount displays (HMD), which are designed to provide full immersion with a rich fusion of the real and virtual worlds, and 2) Informative MR, with smart glasses as a representative product, prioritizing simplicity usability and cost.

While considerable progress has been made, HDMs have yet to achieve the goal of full immersion as originally envisioned. Smart glasses, on the other hand, are more practical in their approach, focusing on simplicity, usability, and affordability.

MEMS Mirrors play a crucial role in imaging formation for both categories of MR products. They are used to deliver images (foveated rendering) to each eye separately, which means that at least two mirrors are required per product. Additionally, MEMS mirrors are used for eye tracking and 3D scanning, meaning that some HMD products may incorporate up to eight MEMS mirrors. Fig. 11 provides an example of smart glasses designed by Bosch [46]. Fig. 11a illustrates how the temple of the smart glasses is utilized to integrate the entire electronics. Fig. 11b shows the temple hinge where the MEMS mirror is placed, while Fig. 11c depicts the lens of the glasses, where the visual information is displayed. In this design, four one-dimensional mirrors are used per pair of smart glasses.

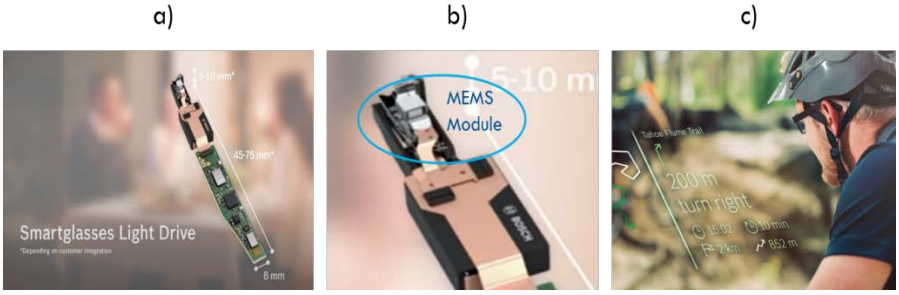

Fig. 11. a) electronics is incorporated in temples, b) MEMS mirror module is located at the hinge of the temple, c) smart glasses use lenses for smart messaging display.

3.4 FSOC Applications

Free space optical communications (FSOC) use high-frequency modulated optical beams for sending data back and forth between optical transceivers [47]. Line of sight (LOS) is essential for FSOC. This technology offers high transmission rates (large bandwidth), lower power consumption (almost half that of RF communication technology), and reduced equipment dimensions (1/10th of the diameter of an equivalent distance/bandwidth RF antenna or even smaller) [48,49]. FSOC is easy to install and license-free, unlike RF standards. This also relates to the fact that the communications are secure as they are directed and broadcasted only toward intended recipient and difficult to intercept. Because of these advantages, it is one of the front runners for broadband link deployment in many space and terrestrial use cases. Typically, FSOC operates in the infrared range at ~1520nm-1560nm due to better eye-safety, and possibility to operate laser at higher power. It should be noted that early development of FSOC

began more than 50 years ago, for applications in the space and defense industry in the US, and in the recent 10 years MEMS mirrors have often become integral part of the system solution [50] as they enable significant overall reduction in system size and cost.

While FSOC is typically focused on space (satellite-to-satellite, satellite-to-earth) applications, and more recently drone applications, there is also strong interest in terrestrial applications. Namely, FSOC is considered as a good solution for the last mile communication in urban areas [47,51]. Additionally, FSOC can be used for connections of Local Area Networks (LANs), Metropolitan Area Networks (MANs), or to support backhaul network for mobile wireless and optical fibers networks. Unfortunately, FSOC also has disadvantages, the most significant being its susceptibility to bad weather conditions, which can degrade the communication link [51]. The FSOC laser signal may get absorbed and scattered by tiny particles, such as aerosols, smoke, dust, and haze [52]. However, practical data indicate that actual down-time is only a few percent of the time, which is acceptable for many difficult to access areas lacking communication infrastructure.

A few examples of successful developments and applications as well as rendering of some applications are shown in Fig. 12. An excellent example is MEMS mirror based compact laser terminal developed by Deutsches Zentrum für Luft- und Raumfahrt, shown in Fig.12b, that was used in pioneering launch of a compact satellite [53]. Another good example would be the FSOC success is GoogleX's Taara project [54, 55]. GoogleX has developed Project Taara as a high-speed cost-effective FSOC system for installation in underdeveloped areas. It can be deployed in rural and difficult to access areas, as well as in urban areas as a last mile extension. The range of the system is 20 km, and it provides speeds of 20 Gbps. Other advantages are low cost, fast and easy deployment, and low environmental impact. Taara products have been already installed in 13 countries. Fig. 12.c shows installation of a Taara FSOC transceiver.

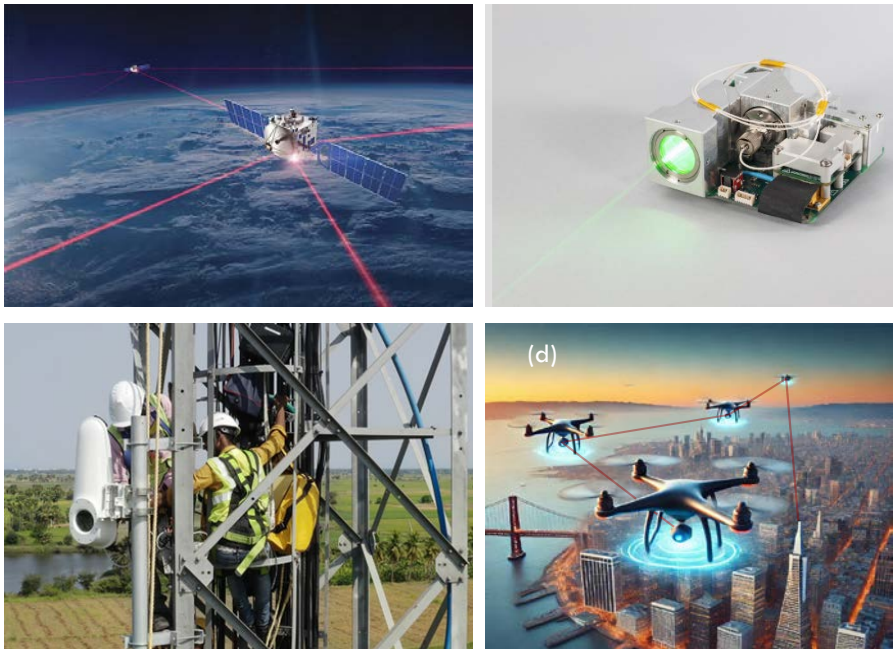

Fig. 12. Examples of FSOC applications with laser beam steering solutions: a) rendering of satellite-to-sattelite FSOC use case with multiple transceivers per satellite, b) MEMS mirror based compact laser terminal by Deutsches Zentrum für Luft- und Raumfahrt , c) Taara FSOC terminal installation, and d) rendering of drone-to-drone and drone-to-infrastructure FSOC application.

3.5 Optical Switching Applications in Data Centers

Artificial Intelligence (AI) will be one of the key driving forces in the next decade, fueling unprecedented demand for data centers and the infrastructure networks that connect them. One of the primary requirements for efficient AI is a development of sophisticated learning models fueled by large datasets. These models demand seamless, simultaneous connectivity across numerous data centers without dropping a single link. This, in turn, necessitates the deployment of ultra-reliable, high-speed switching networks.

Optical switching is emerging as one of the key technologies to revolutionize data networks. As opposed to traditional electronic switching, optical switching eliminates the need to convert light into electrical signal and then back into light, thereby reducing latency and energy consumption. This makes it particularly promising for AI-driven applications and hyperscale datacenters, where massive amount of data requires seamless, instantaneous connectivity, and the energy demand of data centers is a significant concern.

The concept of optical switching using MEMS Mirrors has been described by multiple authors [56,57] more than 20 years ago. Most recently Google has successfully

commercially adopted optical switching with what they call Optical Circuit Switching (OCS) [58]. A MEMS mirror array is at the core of this technology, allowing hundreds of fiber cables to be connected directly to each other without the need for optical-to electrical-to optical conversion. Here MEMS mirrors simply redirect the optical signal, eliminating the need to decode the data packet. Fig.13 illustrates the basic principle of switching between arrays of MEMS mirrors used in the data center network. However, several challenges related to yield, space and cost remain when using Google's approach. We have proposed a modified method utilizing 3D heterogenous integration of MEMS mirrors to form an array [59], which would further improve yield, reduce space, and lower power consumption.

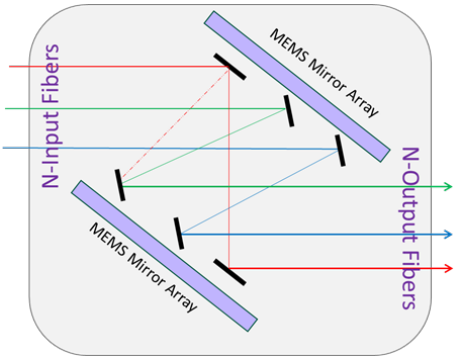

Fig. 13. Optical cross-connect switching using array of MEMS mirrors.

Additionally, a wireless version of optical switching based on MEMS mirrors has been demonstrated for interconnecting servers in data centers [60]. Based on these demonstrations and already commercialized application mentioned earlier, MEMS mirrors are expected to play a center role in optical switching networks for data centers.

3.6 Robotics Applications

Robots and drones are changing our lives and transforming the entire industrial and service sectors, including manufacturing, transportation, automotive, health, and agriculture segments. The integration of robotics in many of these areas improves operations and reduces operating costs. A massive deployment of autonomous mobile robots and drones improves space optimization, efficiency, process control, as well as delivery. At the same time, the introduction of robotics in the work environment creates a new dynamic between the human workforce and machines. Interaction and intention communications between them are frequently required and absolutely critical for safety.

Existing human-machine interaction solutions in the working environment are often based on sound or simple flashing light signals [61]. However, working conditions in manufacturing facilities and warehouses are typically very loud and noisy, and on top of that, they often employ bright light. This significantly hinders human-machine

interaction based on sound or inefficient light messaging. An alternative approach based on MEMS VGLP is proposed in [62]. As shown in Fig. 14, programmable visual messaging can be used for efficient interaction, whereby custom messaging can be clearly displayed. This enables the robot to signal its intentions for its next move or communicate instructions to humans. The proposed VGLP solution is optimized for robotics, offering low power consumption, low weight, small form factor, and high-contrast messaging, outperforming any other existing technology.

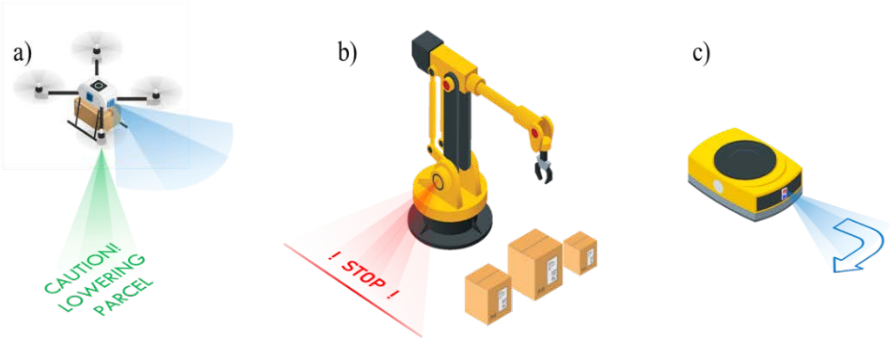

Fig. 14. Programable visual messaging in robotics. a) drone signals intention, b) robot warns for not coming closer, c) robot vacuum cleaner signals intention to move left.

3.7 LiDAR Technology: A Possible Path to Mass Adoption

LiDAR (Light Detection and Ranging) systems have been in the spotlight over the last decade primarily due to the hype surrounding autonomous driving and the expectation that they would become one of the crucial enablers of that technology. However, the high expectations, delays in the widespread adoption of autonomous driving, and inadequate maturity of LiDAR technology have led to disappointment, prompting a reevaluation of LiDAR in the industry.

In this section we provide a high-level analysis of LiDAR technology and outline a potential path to future success.

Why LiDAR in the first place? LiDAR is an active device that senses its surroundings by emitting laser light into an area of interest and measuring the distance to objects in the area of interest. It does so by analyzing the laser beam reflected from the object [63]. LiDAR can generate a three-dimensional representation of its surroundings, hence the term 3D perception sensing, by steering the laser beam in two dimensions and capturing distance or range data (third dimension). LiDAR is more precise than radar in object detection and has an advantage over cameras, as cameras typically lack depth-sensing capabilities. However, LiDAR also has drawbacks – its performance deteriorates in bad weather conditions (rain, snow, fog, dust).

LiDAR Architecture. The high-level architecture of LiDAR is shown in Fig.15. The first insight is that LiDAR is a rather complex system consisting of multiple distinct

blocks. The selection of each component plays a critical role in determining both the system's final performance and its overall cost.

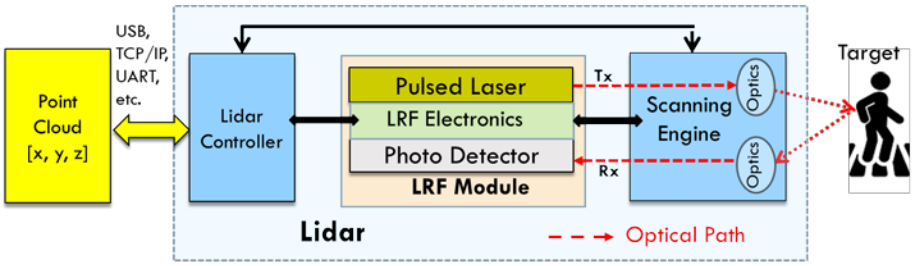

Fig. 15. High-level LiDAR Architecture.

The critical blocks of a LiDAR system are laser source, scanning engine, photo detector, LRF electronics (laser range finder), and optics. The basic principle of operation is as follows: The pulsed laser sends a transmitting beam via the scanning engine and transmission optics into the surrounding space. When the laser beam hits an object, it reflects back and, via the receiving optics, it reaches the photo detector. The number of photons detected depends on the distance. The electronics compare the transmitted and received signals and didact information about the distance. That information, combined with the scanning position, gives a point cloud. The entire process is repeated at scanning rates from Hz to MHz to create a 3D perception image, that represents the scanned environment. Let us now examine the critical functional blocks, starting with lasers.

Laser Source and Wavelength. A laser beam is emitted by a device known as a laser diode, often simply called laser. These lasers are typically classified into two groups based on their lasing mechanism: edge emitter laser (EEL) and vertical cavity surface emitting laser (VCSEL) [64]. EELs emit a laser beam in an elliptical shape from the edge of device, whereas VCSELs emit a circular-shaped laser beam from the surface of the device. EELs are a more mature technology and have been in use for decades. VCSELs, on the other hand, are a newer technology but offer easy creation of two-dimensional array on a single chip, and that is how they are generally used. Both types of lasers operate in pulsed mode. VCSELs typically consume higher power in LiDAR applications compared to EELs.

Lasers used in LiDAR operate in infrared wavelength regions. The most commonly used wavelengths today are between 850 nm and 905 nm, classified as Near Infrared (NIR), and 1550nm, which falls into the Short-Wave Infrared (SWIR) category. NIR lasers are more technologically mature than SWIR lasers. On the other hand, NIR lasers are closer to the visible light spectrum and more dangerous to the human eye when operated at high power. In contrast, 1550 nm lasers, being father from the visible spectrum, can be operated at higher power levels with lower eye safety concerns. When selecting a wavelength, one must also consider laser performance under adverse weather conditions [65,66]. The presence of particles in the air scatters and absorbs

photons and degrades LiDAR performance. NIR lasers are less affected by adverse weather conditions compared to lasers operating at 1550nm wavelength.

Photodetector. A photodetector is a device that converts optical signals into electrical signal, through a phenomenon known as the photoelectric effect. Photosensitivity is very important characteristics of photodetectors, and it depends on the wavelength; therefore, the choice of photodetector is closely related to the choice of laser. An excellent review on the subject is presented in [67]. The most common photodetectors used in LiDAR are Avalanche Photo Diode (APD), Single-photon Avalanche Diode (SPAD), and Silicon Photomultiplier (SiPM). APDs have a current-gain of around 100, low noise, and they are well established, making them widely used in LiDAR systems. The photosensitivity of silicon APDs spans through the visible region of up to 1000 nm, making them unsuitable for 1550 nm wavelengths. To pair them with SWIR lasers one needs to choose indium gallium arsenide (InGaAs) APDs, which, while effective, are more expensive than silicon APDs.

SPADs are popular due to their ability to detect only a few photons within a short period of time. They have an exceptional gain in the order of 10^6, allowing them to detect weak photo signals over long distances. Since they are manufactured using the CMOS process, it is easy to design SPAD array on a single chip.

SiPMs operate on the same principle as SPADs do but can count photons and provide information on the magnitude of the photon flux. This is achieved by designing a dense array of microcells, each composed of paired SPADs. Because of the increased complexity, they are more expensive.

LRF Electronics. Laser Range Finder is a method used to measure distance to an object by using a laser beam. The way the laser beam is modulated defines the type of electronics. Two methods are most commonly used today: 1) Time of Flight (ToF) Method [68], also known as direct detection and 2) Frequency Modulated Continuous Wave (FMCW) Method [69], also known as coherent detection.

ToF Method uses a pulsed laser to determine the distance to an object. It predominantly uses NIR wavelength and is a simpler method between the two in terms of structure and signal processing. Because of the simplicity, ToF is the dominant technology in the market today. However, to increase the range in ToF system requires increasing the laser power, which is not desirable due to eye safety concerns. So, there is a tradeoff that needs to be made.

FMCW operates by constantly emitting frequency-modulated laser signal toward an object while maintaining a reference signal locally (as a local oscillator). The reflected signal from the object is then mixed with the local oscillator signal, producing an intermediate frequency. Using the intermediate frequency and the shift in frequency due to Doppler effect, both the distance and velocity of the object can be simultaneously determined. FMCW is a more complex method, but it offers the advantage of providing additional information on the velocity of the targeted object.

Scanning Engine. The Scanning Engine, also called the Scanning Method, describes how the transmitting laser beam is steered to explore the area of interest. Scanning engines can be classified into mechanical and solid-state types.

Mechanical scanning techniques [70] use bulky rotating mirrors to steer the laser beam through rotation. The most popular mechanical systems use spinning mechanisms with polygonal mirrors and motors. While these systems are bulky and prone to vibration-induced failures, they provide a full 360^0 horizontal field of view.

Solid-state scanning refers to devices used for laser steering that are embedded in the silicon chip. The most common solid-state method involves using a MEMS mirror for laser beam steering. In this case, the MEMS mirror steers the beam following a programmed scan trajectory. Advantages of MEMS-based LiDAR include a small form factor, low power consumption, high reliability of silicon MEMS mirrors, and the ability to dynamically change the field of view, as we have discussed in [71]. This reference also provides an extensive overview of various LiDAR architectures and discussed various trade-offs and uses of MEMS Mirrors.

Flash scanning [72], another solid-state technique, uses a combination of a single laser and an optical diffuser to illuminate the entire scene of interest at once. This technique requires a corresponding photodetector, consisting of a two-dimensional array of photodiodes to capture reflecting returns. In this case, a major drawback is the high laser power required to illuminate the entire scene simultaneously. As a result, flash LiDAR is mainly suitable for short range detection of less than 10m. Another limitation is the restricted field of view defined by optical diffuser. On the positive side, flash scanning eliminates challenges associated with moving laser beam.

Additionally, there are emerging scanning techniques such as optical phase array (OPA) [73,74] where steering of the laser beam is achieved through phase modulation. However, this technology is still far away from maturity, and it will require some time before gaining traction.

Optics. Optics systems are made of lenses, and they play an important role in LiDAR architecture - many would say a crucial role, and they are correct. Lenses are used on both sides of LiDAR: on the transmitter side and on the receiver side. It is important to understand that lenses need to be tailored to specific requirements that depend on the architecture of the LiDAR [75]. Advanced technology plays a prominent role in designing and manufacturing optics for LiDAR. CAD tools such as ZEMAX are frequently used [76], along with advanced materials and coatings, to achieve the desired field-of-view (FOV) and performance with minimal distortion.

The Specific requirements imposed on lenses stem from the function they play in the LiDAR architecture. For example, in ToF LiDAR, the role of the lenses on the transmitter side is to focus the laser beam and keep it collimated (maintaining the beam diameter over distance with minimal divergence), while the role of the lenses on the receiver side is to collect as many photons as possible and focus them onto photodetector. In the case of Flash LiDAR, the lenses on the transmitter side are used to distribute light uniformly over the entire field of view, ensuring uniform illumination of the scene, while the lenses on the receiving side are optimized to focus reflected light onto the array of receiving detectors, enabling a high resolution image from the scene.

In summary, lenses for LiDAR play a critical role in defining FOV. They must be customized to the requirements of the particular architecture. To achieve the desired performance, they may incorporate aspherical surfaces, diffractive elements, or multi-element configurations optimized for specific scanning patterns. All of this underscores that optics indeed plays the crucial role in the LiDAR design.

Software and Data Processing. In LiDAR systems, software and data processing are equally important as hardware. The software synchronizes laser operation with the scanning engine while also managing the scanning pattern. Once data is obtained from the reflecting laser beam, the software processes the data to generate a 3D point cloud or a 2D image representing the scanned area. It often uses advanced algorithms to enhance the data output by filtering noise and correcting distortions, atmospheric effects, and drift over time and temperature. It also offers programmability in operation due to its ability to zoom-in to specific areas of interest. A good example of custom software developed for Lidar is shown in [71].

LiDAR is often integrated with sensing systems such as camera, radar, inertial sensors, or magnetic field sensors, in which case the software fuses data to augment the quality of results (see the section on data fusion). Finally, with the rise of AI, it is expected that machine learning and other smart algorithms will play ever increasing role in interpreting the LiDAR data.

LiDAR's path to mass adoption. Having reviewed the various functional blocks and technologies involved in building a LiDAR system, an important question remains: What is the optimal path to enable the massive adoption of LiDAR? As always, the answer lies in achieving an acceptable cost while maintaining satisfactory performance.

Can we bring the cost down to between $50 to $100? Can power consumption be brought down to approximately 1W? Can the system be miniaturized to matchbox size and weigh less than 50g? We believe the answer is emphatic YES to all these questions. While such a solution may not meet the requirements of every application, it would certainly be suitable for many.

Let us outline a viable path toward low-cost, high-adoption LiDAR. It involves the following choices: Mature EELs, a wavelength range of 850 nm to 905 nm, scanning by MEMS mirrors, and the use of APDs as photodetectors. What do all these choices have in common? They are all mature, well-established technologies. These technologies, combined with the ToF method, could easily push LiDAR manufacturing to millions of units, which would further drive cost down. An example of MEMS LiDAR that follows the proposed path for high adoption and low cost has already been prototyped [71] (see Fig.16). Its architecture is neither strictly monostatic or bistatic, but instead hybrid: consisting of two MEMS Mirrors—one for the transmitting path and one for the receiving path. These mirrors operate as a synchronized pair, hence the name Synchronized MEMS Pair LiDAR (SyMPL). This architecture significantly simplifies the coaxial design and increases its efficiency. SyMPL operates at wavelength of 905nm, leveraging the maturity of EEL technology while benefiting from reduced susceptibility to adverse weather conditions. It is compact (Fig. 16a) and well-suited for further miniaturization, with the potential to be scaled down to the size of a matchbox. The power

consumption of SyMPL is approximately 1W. Designed as a mid-range LiDAR, it has a target range of up to 25 m and FOV of 30º.

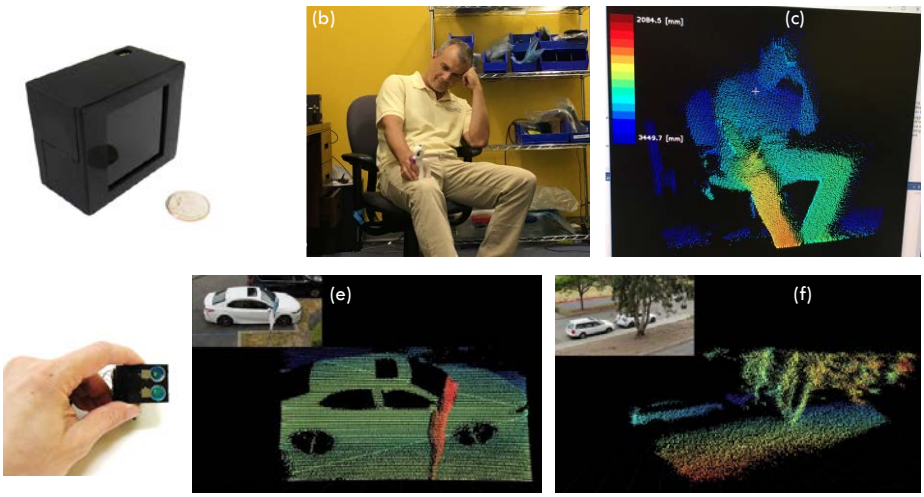

Fig. 16. a) MEMS LiDAR branded as SyMPL, b) "The Thinker" scene, c) SyMPL point cloud data from "The Thinker" scene after removal of background data, d) OEM version of SyMPL MEMS Lidar without housing weighing 49g, e) point cloud of parked car and street sign at ~15m, f) cars and tree at 20m.

We are first to acknowledge that low-cost LiDAR will not solve all problems, and there will always be room for alternative and additional fusion solutions to coexist. However, this approach could be compelling for many applications and it may indeed pave the way for the widespread adoption of LiDAR *en masse*.

3.8 Data Fusion

Data fusion, often called sensor fusion, refers to the simultaneous processing of data from multiple sensors to generate synthesized information of greater intelligence than what individual sensors can provide. Typically, advanced algorithms and special filtering techniques, such as Quaternion Kalman Filtering, are used to produce more intelligent results. A good example of sensor fusion is the integration of signals from an accelerometer, gyroscope, and magnetometer in a smart telephone [77]. By processing these signals together, sensor fusion compensates for the limitation of individual sensors, resulting in more reliable and high-quality information.

The concept of data fusion could also be applied in the optoelectronics space. A promising application is the fusion of LiDAR 3D environmental sensing capability with VGLP technology [62], aimed at enhancing performance and improving safety in application. Fig.17 illustrates the high level concept of this fused solution, referred to as PLidar. As shown in Fig. 17a, PLidar integrates LiDAR with the VGLP projector (Playzer) to enable low-latency, animated visual messaging. In this scenario, as a robot

moves, the LiDAR component scans its surroundings, collects data, and continuously updates the system. Simultaneously, the VGLP projector displays real-time information, such as the robot's angle and distance from a wall (Fig.17b). The AI model processes LiDAR data and dynamically streams messages, ensuring reliable and real-time updates. The tight interaction between sensing and display significantly enhances workplace reliability and safety. Similarly, as depicted in Fig.17c, a humanoid robot can leverage data fusion to scan its surroundings using LiDAR and project tailored messages onto the ground, facilitating enhanced robot-human interaction. Additionally, by utilizing facial recognition based on LiDAR data, the system can identify individuals, further expanding its potential applications.

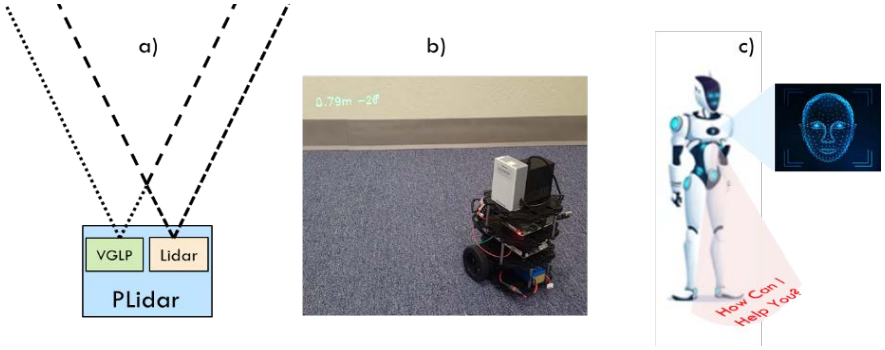

Fig. 17. a) Fusion of VGLP capability with Lidar sensing capability creates PLidar, b) PLidar in action assembled on the mini robot, c) PLidar enhancing humanoid robot capabilities.

One can envision the use of this technology in various other applications. For example, in the automotive space, a system integrating radar with VGLP projection could enhance pedestrian safety. In this scenario, the radar detects pedestrians around the vehicle, while the VGLP projector displays visual warnings directly onto the ground, alerting them not to cross the vehicle's path. This real-time interaction between sensing and display improves pedestrian-vehicle communication, ultimately enhancing safety and reducing accident risks.

4 Can MEMS Mirrors Reach One Billion Units?

It is evident from the discussion in this paper that MEMS Mirror applications are numerous (Fig.18), and we are not even scratching the surface. Many of the outlined applications are expected to generate billions of dollars. We will mention just a few to illustrate the point. MR devices, which are predicted to capture market share from smart phones, are expected to grow to hundreds of millions of units pushing this market segment to billions of dollars. The same applies to optical switching in data centers, driven by the insatiable demands from AI. Additionally, autonomous Robo-taxis, with numerous LiDARs distributed around the vehicle, represent another market opportunity of billions of dollars. On top of this, many new applications will emerge - some of which

we cannot yet foresee. Taking all of this into account, one can estimate that market opportunities for MEMS Mirrors will reach tens of billions of dollars in the next decade.

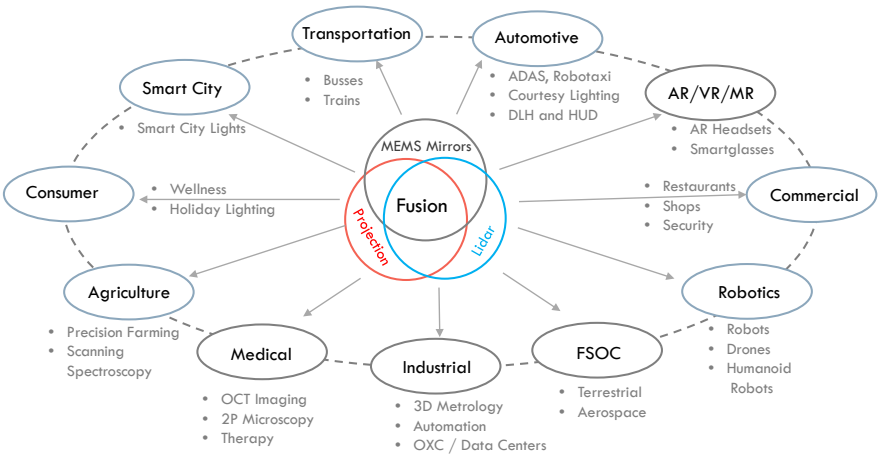

Note: DLH – Dynamic Laser Headlights, HUD – Head Up Display, MR – Mixed Reality (AR/VR), FSOC – Free Space Optical Communication, OCT – Optical Coherence Tomography, OXC – Optical Cross Connect Switching

Fig. 18. MEMS Mirrors applications are numerous, and market opportunities will amount to billions of dollars.

Status of MEMS Mirrors technology. After two decades of development, MEMS mirrors are entering a phase of maturity. These devices are very reliable since they are made out of silicon crystal. Extensive testing and data have shown the ability to operate over a billions of cycles without failure. When we consider the numerous applications, some of them described here, it becomes clear that the conditions are right for exponential growth in the next decade and that the path to reaching a volume of billion units annually is entirely feasible. The confidence level is further reinforced by the fact that multiple groups of MEMS products have already followed a similar trajectory (Fig.19).

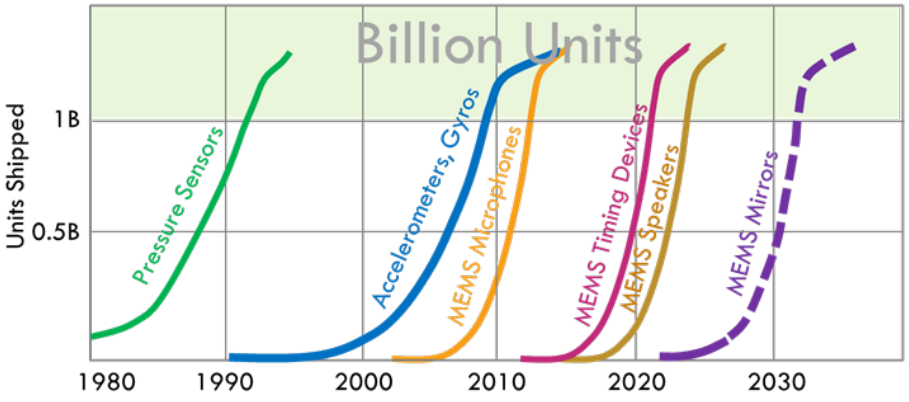

Fig. 19. MEMS mirrors – the next big wave in MEMS technology. Products from pressure sensors to speakers have already reached shipments of more than billion units annually.

5 Summary

We have reviewed MEMS technology, tracking its multiple successes that have led to its emergence as a mainstream solution for delivering reliable products in high volumes. Several product categories have already reached production volumes in the billions, attesting to the robustness and credibility of this technology.

Our analysis of MEMS mirror technology underscores the maturity of these devices, which are now on the cusp of entering a high-growth phase and are poised to replicate the success of their MEMS predecessors. Additionally, we examined the current state of LiDAR technology and proposed a potential path forward for its widespread adoption centered on MEMS LiDAR architecture.

Based on our overall analysis, we concluded that MEMS mirrors are well positioned to reach an annual production volume of one billion units in the next decade, with market opportunities valued in the tens of billions of dollars.

References

1. Petersen, K.E.: Silicon as a mechanical material, Proceedings of the IEEE, 70 (5), 420-457, May (1982); doi: 10.1109/PROC.1982.12331.
2. Howe, R.T. and Muller, R.S.: Polycrystalline silicon micromechanical beams, Journal of the Electrochemical Society, 130, pp. 1420-1423 (1983).
3. Ristic, Lj., Hughes, H., and Shemansky, F.: Bulk Micromachining Technology, ch.3. In: Ristic, Lj., (ed.), Sensor Technology and Devices, Artech House, Boston (1994).
4. Ristic, Lj., Shemansky, F., Kniffin, M.L., and Hughes, H.: Surface Micromachining Technology, ch.4, In: Lj. Ristic (ed.), Sensor Technology and Devices, Artech House, Boston (1994).
5. Ristic, Lj.: CMOS technology: a base for micromachining, Microelectronics Journal, 20, (1–2), 153-169 (1989), ISSN 1879-2391; https://doi.org/10.1016/0026-2692(89)90128-6
6. Tang, W.C., Nguyen, T.-C. H., and Howe, R.T.: Laterally driven polysilicon resonant microstructures," Sensors and Actuators, 20, pp. 25-32 (1989).
7. Patent US5146389, Differential capacitor structure and method, 1992-09-08.
8. Ristic, Lj. et al.: A capacitive type accelerometer with self-test feature based on double-pinned polysilicon structure, 7th Int. Conf. SSSA, Transducers '93, Yokohama, June (1993).
9. Patent US5181156, Micromachined capacitor structure and method for making, 1993-01-19
10. Patent US5545912, Electronic device enclosure including a conductive cap and substrate, 1996-08-1.
11. Vujosevic, M., Shah, M.: Stress isolation of an accelerometer die in a post-molded plastic package--The impact of die coat coverage. In: SAE Technical Paper Series 1999, SAE International Congress and Exposition, Detroit, Michigan, March 1-4 (1999).
12. Patent US5632854, Pressure sensor method of fabrication, 1997-05-27
13. Smith, S. C.: Piezoresistance Effect in Germanium and Silicon, Phys. Rev., 94, p.42, (1954)
14. Kasten, K. et al.: Capacitive pressure sensor with monolithically integrated CMOS readout for high temperature applications, Sensors and Actuators A: Physical, 97-98, pp.83-87 (2002)

15. Stoler, A. I.: The Etching of Deep, Vertical-Walled Patterns in Silicon, RCA Rev., 31, p.271 (1970)
16. Wagner, H. A.: Electrochemically Controlled Thinning of Silicon, Bell. Syst. Tech. J.50, p.473 (1970)
17. Bean, K. D.: Anisotroping Etching of Silicon, IEEE Trans. El. Dev., ED-25, 1185 (1978)
18. X-ducerTM Sensor Element, in Motorola, Sensor Device Data Book, DL 200/D, Rev.5, 01/2003, Motorola Pressure Sensors, p.3-8 (2003)
19. Hertz, J.: STMicroelectronics Debuts 'First' Waterproof MEMS Pressure Sensor, All About Circuits, June 5 (2023); https://allaboutcircuits.com/news/st-debuts-first-waterproof-mems-pressure-sensor/
20. Gogoi, B., Vujosevic, M., and S. Petrovic,: Challenges in MEMS Packaging, Invited paper, SMTA International Congress and Exposition, Chicago, Illinois, 24-38 September (2000).
21. Frank, R., Kniffin, M.L., Ristic, Lj.: Packaging for Sensors, ch.6, p.233, in Ristic, Lj. (ed.), Sensor Technology and Devices, Artech House, Boston (1994).
22. Bever, T., Kandler, M.: Solutions for Tire Pressure Monitoring Systems, in Valldorf, J., Gessner, W. (eds.) Advanced Microsystems for Automotive Applications, pp. 261-269, Publisher Name: Springer, Berlin, Heidelberg (2003); doi.org/10.1007/978-3-540-76988-0_21
23. Freescale introduces world's smallest integrated tire pressure monitoring system, Green Car Congress, 20 Oct. (2014); https://www.greencarcongress.com/2014/10/20141020-freescale.html
24. Adorno, S., Cerini, F., Vercesi, F. (2022). Microphones. In: Vigna, B., Ferrari, P., Villa, F.F., Lasalandra, E., Zerbini, S. (eds), Silicon Sensors and Actuators. Springer, Cham. https://doi.org/10.1007/978-3-030-80135-9_15.
25. Inoue, T., Udhida, Y., Ishimoto, K. and Horimoto, Y.: Study and development of low-noise MEMS acoustic sensors. OMRON TECHNICS Vol.50.012EN (2019).
26. Wenzel, T, and Retting, R.: Design of MEMS Microphone Protective Membranes for continuous outdoor applications. Applied Acoustics, 183, December (2021), https://doi.org/10.1016/j.apacoust.2021.108304.
27. Wasisto, H.S., Anzinger, S., Acanfora, G. et al.: Acoustically semitransparent nanofibrous meshes appraised by high signal-to-noise-ratio MEMS microphones. Commun Eng 3, 136 (2024). https://doi.org/10.1038/s44172-024-00283-4.
28. Patent CN112492489B, Waterproof MEMS microphone, 2022-06-24.
29. Seo, K.; Park, J.; Kim, H.; Kim, D.; Ur, S.; Yi, S.: Micromachined piezoelectric microspeakers fabricated with high quality AlN thin film, Integr. Ferroelectr. 95, 74–82 (2007)
30. Sturtzer, E., Shahosseini, I., Pillonnet, G., Lefeuvre, E,, Lemarquand, G.: High fidelity microelectromechanical system electrodynamic micro-speaker characterization. J. Appl. Phys. 113, 214905 (2013).
31. Garud, M.V., Pratap, R.: A novel MEMS speaker with peripheral electrostatic actuation. J. Microelectromechanical Syst., 29, 592–599 (2020).
32. Fei, W., Zhou, J., Guo, W.: Low-voltage driven graphene foam thermoacoustic speaker. Small 2015, 11, 2252–2256 (2015).
33. Gazzola, C., Zega, V., Cerini,F., Adorno, S., and Corigliano, A.: On the Design and Modeling of a Full-Range Piezoelectric MEMS Loudspeaker for In-Ear Applications. J. of Microelectromechanical Systems, 32, (6), 626-637, Dec. (2023); doi: 10.1109/JMEMS.2023.3312254.
34. Van Beek, J.T.M., and Puers, R.: A review of MEMS oscillators for frequency reference and timing applications. J. Micromechanics and Microengineering, 22 (1), 013001 (2012); doi: 10.1088/0960-1317/22/1/013001

35. Chen, C.Y., Li, M.H., Li, S.S.: CMOS-MEMS Resonators and Oscillators: A Review, Sensors and Materials, 30 (4), 733-756 (2018)
36. Lutz, M., Partridge, Tabatabaei, A.S., and Sevalia, P.: Programmable MEMS-based silicon timing solutions change the game. NSTI-Nanotech 2011, www.nsti.org, ISBN 978-1-4398-7139-3, vol.2, (2011).
37. Partridge, A., and McDonald, J.: MEMS to replace quartz oscillators as frequency sources. NASA Tech Brief, vol.30, (6), (2006).
38. Milanović, V., Matus., A.G., McCormick, D.T., Gimble-Less Monolithic Silicon Actuators for Tip-Tilt-Piston Micromirror Applications, IEEE J. Sel. Topics in Quantum Electronics, 10 (3), 462-471 (2004).
39. Milanović, V., Multilevel-beam SOI–MEMS fabrication and applications, J. Microelectromech. Syst., 13 (1), 19–30, Feb. (2004).
40. Ristic, Lj.: MEMS mirrors: The next big wave in MEMS technology, Laser Focus World, July, (2023), https://www.laserfocusworld.com/optics/article/14296740/mems-mirrors-the-next-big-wave-in-mems-technology
41. https://www.mirrorcletech.com/wp/products/mems-mirrors/
42. https://www.mirrorcletech.com/wp/products/system-solutions/playzer/
43. Kasturi, A., Milanović, V., Hu, F., Kim, H. J., Ho, D., Lovell, D.: MEMS Mirror Module for Programmable Light System, SPIE 2019 OPTO Conf., San Francisco, CA. February 3, (2019)
44. Azuma, R.: A Survey of Augmented Reality. In Presence: Teleoperators and Virtual Environments, 6 (4), 355-385, Aug. (1997).
45. Azuma,R. Hoff, B., Neely, H., and Safarty, R.: A Motion-Stabilized Outdoor Augmented Reality System. In: Proc. IEEE Virtual Reality '99. Houston, 252-259, TX, 13-17 Mar. (1999).
46. Smartglasses Light Drive | Bosch Sensortec; https://www.bosch-sensortec.com/products/display-solutions/smartglasses-light-drive/
47. Leitgeb, E., Gebhart, M., and Birnbacher, U.: Optical Networks, Last Mile Access and Applications, Journal of Optical Fiber Commun. Res., 2(1), 56–85, (2005).
48. Chaleshtory, Z.N., Gholami, A., Ghassemlooy, Z., Sedghi M.: Experimental Investigation of Environment Effects on the FSO Link with Turbulence. IEEE Photon Technol Lett (2017) 29:1435–8. doi:10.1109/LPT.2017.2723569.
49. Hong, Y-Q., Kwon, D-H., Choi, J-Y., Ha, I-H, Shin, W-H, Han, S-K.: SOA-based Multilevel Polarization Shift On-Off Keying Transmission for Free-Space Optical Communication. Photonics (2021) 8:100–8. doi:10.3390/photonics8040100.
50. Kingsbury, R. W. et al.: Fast-Steering Solutions for Cubesat-Scale Optical Communications, ICSO 2014, Tenerife, Canary Islands, Spain, 7 – 10 Oct. 2014; https://dspace.mit.edu/bitstream/handle/1721.1/132241/105630G.pdf?sequence=2&isAllowed=y
51. Hammel, F. D. Eaton and S. L. Lachinova.: Atmospheric Channel Effects on Free-Space Laser Communication, Journal of Optical Fiber Communications, vol. 3(2), 111–158, (2006).
52. Chauhan, S., Miglani, R., Kansal, L., Gaba, G.S., Masud M. Performance Analysis and Enhancement of Free Space Optical Links for Developing State-Of-TheArt Smart City Framework. Photonics (2020) 7:132; doi:10.3390/ photonics7040132.
53. A pioneering launch – compact satellite PIXL-1 carries the world's smallest laser terminal into orbit; https://www.dlr.de/en/latest/news/2021/01/20210124_pioneering-launch-compact-satellite-with-smallest-laser-terminal
54. Taara - A Google X Moonshot; https://x.company/projects/taara/
55. https://taaraprojects.com

56. Bishop, D.J., C. R. Giles, and G. P. Austin,: The Lucent Lambda-Router: MEMS technology of the future here today, IEEE Comm. Mag., 40, (3), 75–79 (2002)
57. Yamaguchi, J. et al.: High-yield fabrication methods for MEMS tilt mirror array for optical switches, NTT Technical Review, 5 (10), Oct. (2007).
58. Urata, R. et al., Mission Apollo: Landing optical circuit switching at datacenter scale, Aug. (2022), https://doi.org./10.48550/arXiv.2208.10041
59. Milanović, V., and Ristic, Lj.: MEMS Mirror Array Optical Switching Technology by Advanced Packaging, Project proposal for U.S. CHIPS and Science Act funding, 2025-NIST-CHIPS-NAPMP-01, December (2024).
60. Deng, P., Kane, T.: Alharbi, O., Reconfigurable free space optical data center network using gimbal-less MEMS retroreflective acquisition and tracking, Proc. of SPIE Vol. 10524 1052403-1, (2018); doi: 10.1117/12.2295831
61. Palinko, O. et al.: Intention Indication for Human Aware Robot Navigation, doi.org/ 10.5220/0009167900640074
62. Lovell, D. et al.: Optical MEMS Enable Next Generation Solutions for Robot Vision and Human-Robot Interaction, Proceedings of the SPIE, vol.12013, MOEMS and Miniaturized Systems XXI, 1201304, March (2022); https:// doi.org/10.1117/12.2613458
63. Li, J., Ibanez-Guzman, J.: Lidar for Autonomous Driving: The principles, challenges, and trends for automotive lidar and perception systems, Apr. 2020, arXiv:2004.08467v1 [cs.RO] 17 Apr (2020).
64. Boucart, J.: Shining a Spotlight on Laser Sources for Automotive Exterior LiDAR, e-motec.net (E-Mobility Technology International), Sept. 15 (2021); https://www.e-motec.net/laser-sources-for-automotive/
65. Michaud, S., J.-F. Lalonde, and P. Gigure, “Towards characterizing the behavior of LiDARs in snowy conditions,” in IEEE/RSJ IROS Workshop on Planning, Perception and Navigation for Intelligent Vehicles, (2015).
66. Kutila, M., Pyykonen, P., Holzhuter,H., Colomb, M., and Duthon, P.: “Automotive LiDAR performance verification in fog and rain,” in 21st IEEE International Conference on Intelligent Transportation Systems (ITSC), (2018).
67. Sun, X.: Review of photodetectors for space Lidars, Sensors 2024, 24, 6620 (2024); doi.org/10.3390/s24206620
68. Li, L.: Time of Flight Camera – An Introduction, Technical White Paper, SLOA190B – January 2014, Revised May (2014)
69. Gao, S.: Hui, R.: Frequency-modulated continuous-wave lidar using I/Q modulator for simplified heterodyne detection, Optics Letters, 37 (11), 2022-2024, (2012); https://doi.org/10.1364/OL.37.002022
70. Raj, T. et al.: A survey on Lidar scanning mechanism, Electronics 2020, 9, 741 (2020); doi.org/10.3390/electronics9050741
71. Kasturi, A. et al.: Comparison of MEMS mirror LiDAR architectures", Proc. SPIE 11293, MOEMS and Miniaturized Systems XIX, 112930B, February (2020), https://doi.org/10.1117/12.2556248
72. Amzajerdian, et al.: “Imaging Flash Lidar for Autonomous Safe Landing and Spacecraft Proximity Operation,” in AIAA SPACE, Long Beach, U.S.A, (2016).
73. Mcmanamon, P.F., et al., “Optical phased array technology,” Proceedings of the IEEE, 84, 268–298 (1996)
74. Acoleyen, V. et al.: Integrated Optical Beam Steerers. In Proceedings 2013 Optical Fiber Communication Conference and Exposition and the National Fiber Optic Engineers Conference (OFC/NFOEC), Anaheim, CA, USA, pp. 6–8, 17–21 March (2013)

75. Argueta, V.: Exploring LIDAR Lens Design: Innovations and Applications in Optical Engineering, OFH, Sept.16 (2024); https://www.opticsforhire.com/blog/lidar-lens-design-optical-layout/
76. Lee, X., Wang, C.: Optical design for uniform scanning in MEMS-based 3D imaging lidar, Applied Optics, 54 (9), 2219-2223 (2015); doi.org./10.1364/AO.54.002219
77. Ristic, Lj.: Sensor fusion and MEMS technology for 10-DoF solutions, EE Times, Sept. 3, (2012).